Spatially and Temporally Controlled Biomineralization Is Facilitated by Interaction between Self−Assembled Dentin Matrix Protein 1 and Calcium Phosphate Nuclei in Solution †

8 AUTHORS, INCLUDING:

D. J. Cookson
Australian Synchrotron
126 PUBLICATIONS   3,301 CITATIONS

SEE PROFILE

Chunlin Qin
Baylor College of Dentistry
140 PUBLICATIONS   3,232 CITATIONS

SEE PROFILE

Spatially and temporally controlled biomineralization is facilitated by interaction between self-assembled dentin matrix protein 1 and calcium phosphate nuclei in solution

Gen He[‡], **Sivakumar Gajjeraman**[‡], **David Schultz**[§], **David Cookson**[§], **Chunlin Qin**[⊥], **William T. Butler**[⊥], **Jianjun Hao**[‡], and **Anne George**[‡]

‡ *Department of Oral Biology, University of Illinois at Chicago, Chicago, IL 60612*

§ *ChemMatCARS, 9700 S. Cass Avenue. Bldg. 434 D Argonne, IL 60439*

⊥ *Department of Basic Sciences, The University of Texas-Houston Health Science Center, Dental Branch, Houston, Texas 77030*

Abstract

Bone and dentin biomineralization are well regulated processes mediated by extracellular matrix proteins. It is widely believed that specific matrix proteins in these tissues modulate nucleation of apatite nanoparticles and their growth into micrometer sized crystals via molecular recognition at the protein-mineral interface. However, this assumption has been supported only circumstantially and the exact mechanism remains unknown. Dentin matrix protein 1 (DMP1) is an acidic matrix protein, present in the mineralized matrix of bone and dentin. In the present study we have demonstrated using synchrotron small-angle X-ray scattering that DMP1 in solution can undergo oligomerization and temporarily stabilize the newly formed calcium phosphate nanoparticle precursors by sequestering them and preventing their further aggregation and precipitation. The solution structure represents the first low resolution structural information for DMP1. Atomic force microscopy and transmission electron microscopy studies further confirmed that the nascent calcium phosphate nuclei formed in solution were assembled into ordered protein-mineral complexes with the aid of oligomerized DMP1, recombinant and native. This study reveals a novel mechanism by which DMP1 might facilitate initiation of mineral nucleation at specific sites during bone and dentin mineralization and prevent spontaneous calcium phosphate precipitation in areas in which mineralization is not desirable.

Keywords

Dentin Matrix Protein 1; Biomineralization; SAXS

Mineralized tissue such as bone and dentin are unique biocomposites of a structured organic matrix impregnated with matrix-oriented carbonated apatite crystals (1). The rigidity and compressive strength of bone and dentin are directly dependent upon temporally and spatially controlled mineral nucleation and hierarchically assembled matrix (2,3). It is well known that biological fluids are metastable or supersaturated with respect to calcium salts i.e., they are below the saturation needed for spontaneous precipitation but are well above the saturation to support crystal growth after the initial nucleus has formed (4,5). Therefore, a driving force is required to lower the activation energy of nucleation and formation of thermodynamically

To whom correspondence should be addressed. (A.G) Tel: 312-413-0738, Fax: 312-996-6044, E-mail: anneg@uic.edu.

stable hydroxyapatite nanocrystals. Compelling *in-vitro* and *in-vivo* data provide evidence that bone and dentin specific noncollagenous proteins play a critical role in the initiation and growth of the calcium phosphate mineral phase (6-8). Although the exact mechanism remains unknown, it is postulated that kinetic control of biomineral crystallization is achieved by interactions between mineral nuclei and soluble or immobilized acidic proteins. Atomic force microscopy indicates that proteins extracted from calcite or aragonite-containing layers of the abalone shell bind to growth sides on well-defined calcium carbonate crystal surfaces and influence the kinetics of crystal growth from solution (9). This protein-mineral interaction might be an essential strategy used by organisms for precipitating the desired polymorph, controlling the structure and composition of the nuclei, particle size, texture, habit and stability of intermediate phases. However, our knowledge on protein-mediated mineralization process at the early stages of crystal nucleation and growth is limited and the molecular interactions at the protein-mineral interface remain poorly understood.

Dentin matrix protein 1 (DMP1) is an acidic noncollagenous phosphoprotein now known to be present in the mineralized matrix of both dentin and bone (10-13). Recent studies have established DMP1 as a multifunctional protein which plays a crucial role in osteoblast/ondotoblast differentiation and mineral nucleation events (7,14 and 15). Circular dichroism analysis has shown that recombinant DMP1 exists as a random coil with no distinct fold (16). However, upon calcium binding, the C-terminal domain adopts a β-sheet secondary structure and gradually self-assembles into oligomers and microfibrils (7). Self-assembly motifs were also identified in DMP1 and these peptides were shown to promote preferred orientation of the nucleated hydroxyapatite (7).

In biomineralization systems, uninhibited mineral precipitation would override the well-regulated nucleating function of anionic proteins and impair the complex textures and morphologies of bone and dentin crystals. Therefore, in the present study small angle X-ray scattering (SAXS) has been used to characterize the process of nascent calcium phosphate nuclei formation in solution and spatially controlled mineral deposition mediated by DMP1. SAXS data was also used to generate low resolution models of DMP1 in the presence and absence of calcium. Atomic force microscopy (AFM) and transmission electron microscopy (TEM) studies further confirmed that the nascent calcium phosphate nuclei formed in solution were assembled into ordered protein-mineral complexes with the aid of oligomerized DMP1, both recombinant and native. AFM could be used to image the nanometer sized assembly of DMP1 in the presence of calcium. Understanding the early stages of mineral nucleation from a supersaturated calcium phosphate solution in the presence of DMP1 should shed light on calcification mechanisms.

Materials and Methods

Purification of recombinant DMP1

DMP1 was expressed recombinantly and purified as described earlier (17).

Preparation of Protein Samples for SAXS

Purified recombinant DMP1 solutions were prepared at a concentration of 2 mg/ml and 5 mg/ml in 10 mM Hepes, 165 mM NaCl and pH 7.4. To evaluate the calcium binding properties of DMP1, the protein solution was mixed with 2 M $CaCl_2$ at a final concentration of 5 mM Ca^{2+} using a stop-flow apparatus. Immediately prior to measurement, the protein samples were filtered through a Millipore membrane (0.2μm pore size).

SAXS Experiments

Synchrotron SAXS experiments were performed at the Synchroton Radiation Facility, Advanced Photon System, Argonne National Laboratory, on beamline in sector 15-ID-D at ChemMat CARS. The wavelength used for the current experiment was 8.00 keV, from a tunable source that produces tunable radiation (6-32) keV. The X-ray beam was monochromated with a double crystal, diamond monochromator with resolution of 10^{-4} Δ_E/E and from the monochromator passed through a double-bounce mirror system with 1:1 focusing with an approximate X-ray source-to-sample distance of ~60 meters. The focusing distance was ~30 meters. Camera length was 1870 mm from the sample and X-ray beam size in the vertical direction was ~150 microns (focused) and ~400 microns in the horizontal. The instrument was equipped with Bruker 6000 CCD detector (130 mm diameter, 92 micron pixel size, 1024x1024 pixels) and samples were mounted in quartz capillaries (1.5 mm).

DMP1 solution was placed in a capillary tube for analysis. Variations in DMP1 concentration (2 μg/ml to 5 μg/ml) resulted in identical SAXS results and therefore DMP1 at a concentration of 5 μg/ml was used for further experiments. BSA (bovine serum albumin) was used as a control.

Calcium binding experiments were performed *in situ* in a time lapse mode. To check for radiation damage, the data were collected in 15 successive frames (1-min) and only the time frames in which the data remained unchanged (i.e. protein was stable against beam radiation) were used for further analysis. The data was normalized and processed, and the scattering of the corresponding buffer was subtracted. The relative scattering intensity was examined from the aged solution containing 10 mM HEPES, 165 mM NaCl, 2.5 mM CaCl , 1 mM KH_2PO_4, 0.5 μg/μl DMP1 which was incubated at 37 °C for 1 month. Buffers without DMP1 were examined simultaneously and served as a control.

Data Evaluation

The experimental SAXS data for all samples were linear in a Guinier plot in the low q region. The forward scattering I (0) and the radius of gyration R_g were calculated by the Guinier approximation (18) and indirect Fourier transform generated by program GNOM (19). This program was also used to compute the pair-distance distribution functions P(r) of the particles. The molecular masses of the solutes were calculated using BSA solution as a standard (20).

Ab Initio Modeling

Low resolution models were generated by the *ab initio* program GASBOR. GASBOR searches a chain-compatible spatial resolution of an exact number of dummy residues, (DRs) which corresponds to the Cα atoms of protein amino acids and uses simulated annealing to build a locally 'chain-compatible' DR-model inside the same search volume (21). The DR modeling is able to better account for the internal structure and generally provide more detailed models than those given by the shape determination algorithms. For each protein with and without calcium, results from at least 10 separate runs were averaged by the package DAMAVER (22) to construct the average model representing the general structural features of all the reconstructions.

Atomic force microscopy analyses

AFM imaging was used to analyze the self-assembly process of DMP1 in the presence of calcium. AFM imaging technique was used. DMP1 (5 μg/ml in 10 mM HEPES, 165 mM NaCl, 2.5 mM $CaCl_2$, pH 7.4) was incubated at room temperature overnight. DMP1 solution (10 μl) was then deposited onto a freshly cleaved muscovite form of mica surface (grade-V). After the sample was adsorbed (10 min), the surface was washed with nanopure water and air-dried. The

sample adsorbed on the mica surface was scanned using AFM (Nanoscope III, Digital Instruments) in the tapping mode, the instrument equipped with D-scanner (scan range of 12×12 μm). Silicon cantilevers (Model # RTESP from Veeco Instruments) were used for all measurements.

Samples were also prepared in pseudophysiological buffer (10 mM HEPES, 165 mM NaCl, 2.5 mM $CaCl_2$, 1 mM KH_2PO_4, 0.5 μg/ml DMP1, pH 7.4) incubated at 37°C overnight and subjected to AFM analysis as described above. Data were collected as topographic and phase images, where the latter is a convolution of topography and tip-sample interactions.

Transmission Electron Microscopy Analysis

For TEM analysis, DMP1 (5 μg/ml) was incubated overnight with the same buffer used for AFM namely (10 mM Hepes, 165 mM NaCl, 5 mM $CaCl_2$, 2 mM KH_2PO_4, pH 7.4) at 37°C. Carbon formavar coated nickel grids were floated on a drop of the above solution (10 min) and washed (3×) with nanopure water. The grids were air dried and imaged by high resolution TEM (JEOL 3010). To increase image contrast the grids were negatively stained with 1% uranyl acid (1 min) and examined by TEM (JEM 1220). The identical experimental setup with the same concentration of BSA or solutions without protein served as controls.

Precipitation of DMP1 by calcium

The precipitation assay (23) was conducted by preparing a buffer solution (10 mM HEPES, 165 mM $CaCl_2$, 2 mM KH_2PO_4, pH 7.4 with 1 mCi/l $^{45}CaCl_2$) and adding DMP1 to a final concentration of 5 μg/ml and 1 μg/ml. Identical solutions of BSA were prepared in parallel as controls along with solutions not containing DMP1. The solutions were incubated at 37°C and at each time point aliquots (50 μl) aliquots were removed, centrifuged at 16,000g for 5 min and the radioactivity in the supernatant quantified using a liquid scintillator. Measurements were performed in triplicate samples and the radioactivities averaged and converted to calcium concentration.

Results

Solution Structure of DMP1 in the absence and presence of calcium

Guinier curves provide the radius of gyration (R_g), defined as the root mean square distance (RMSD) of all atoms from their common centre of mass. The R_g can be used to evaluate the overall shape of a scattering molecule. Based on Guinier plot analyses and indirect Fourier transformation analysis (19), the radius of gyration (R_g) of DMP1 in solution was found to be 3.37 ± 0.01 nm. Based on the intensity at the origin ($I(0)$) calculations, the apparent molecular mass of the DMP1 backbone was determined to be 51 kDa, which is in good agreement with the value predicted from its primary sequence (51kDa).

To determine the structural changes induced in DMP1 by calcium (5 mM), time-resolved X-ray data was collected since SAXS is particularly sensitive to the formation of dimers and higher oligomers of biomolecules. After the introduction of calcium (1 min), no significant change in the molecular weight implied that DMP1 maintained a monomeric state in solution. However, the radius of gyration increased from 3.37 ± 0.01 nm. to 3.73 ± 0.01 nm. Dimerization of the protein was observed 3 min following the introduction of calcium as the apparent molecular mass was twice that calculated from the amino acid sequence. Correspondingly, the radius of gyration increased to 4.85 ± 0.01 nm, implying a higher order organization of DMP1 with the addition of calcium and that the dimer is highly elongated. These changes associated with the above parameters were further supported by changes in the distance distribution $p(r)$ function computed from the experimental data (Fig. 1a). The $p(r)$ function plotted against interatomic distances within the DMP1molecule yielded visual information about its shape

(20). These results demonstrate that the DMP1 molecule assumed an elongated shape based on the extended slope at longer distances, characteristic for elongated particles. The maximal particle dimensions (Dmax) deduced from a Guinier plot for DMP1 in the absence of Ca2+ and following calcium introduction (1min and 3min) were found to be 11.6 nm,13.8 nm and 20 nm respectively (Fig. 1a), implying that the process of dimer formation may be divided into sub-states. Thus the apparent molecular mass and radius of gyration values obtained from SAXS data suggest that DMP1 could undergo oligomerization in solution and form elongated dimers within 3 min after calcium binding.

Ab initio models of DMP1 in solution

To gain further insight into the molecular shape and self-assembly of DMP1 in the presence of calcium, low-resolution protein structures were generated by the *ab initio* program GASBOR, which depicts protein models through the assembly of dummy residues (DRs) and uses simulated annealing to build a locally "chain-compatible" DR-model inside the same search volume (21). DR models are able to depict the internal structure better and in more detail than those determined by the shape determination algorithms (20). Typical *ab initio* models of the partial constructs after repetitive *ab initio* runs for each protein scattering file are displayed in Fig. 1b. From the low- resolution models, it appears that DMP1 adopts an elongated structure, but upon calcium binding (within 1 min) both the Rg and Dmax increased. This first low-resolution model depicts the molecular shape of DMP1 as an extended structure at one end of the molecule with a compact globular domain at the other (Figure. 1b). We have previously demonstrated that the C-terminus of DMP1 exhibits profound conformational changes upon calcium binding, i.e. the conformation shifts from random coil to β-sheet (7). Based on this data, the extended structure has been assigned as the C-terminus and the globular structure as the N-terminus of DMP1. Judging from the molecular mass derived from I (0), DMP1 was shown to undergo extensive dimerization upon calcium binding after 3 min incubation. This result is in good agreement with the generated low- resolution model, which appeared as elongated symmetric DRs, even though no symmetry restrictions (P1) were set during the annealing procedure. Such an elongated molecule accompanying DMP1 dimerization can only be attained by C-terminal mediated interactions. Overall, the data processed by *ab initio* methods confirm that DMP1 form a dimer in solution, yielding a symmetric two-domain structure. This model is in good agreement with our earlier studies (7) and represents the first low resolution structural information for DMP1 in the presence and absence of calcium.

Characterization of calcium induced DMP1 self-assembly

We had demonstrated earlier, that acidic peptides located at the C-terminus of DMP1 could oligomerize and gradually form well-aligned microfibrils in the presence of calcium (7). To further explore the mechanism involved during the formation of this precursor phase, AFM was used to monitor the self-assembly process of both recombinant DMP1 and the 57 kDa fragment from the carboxyl terminal of native DMP1in the presence of calcium. Fig 2B shows that DMP1 can self-assemble into nanometer-sized clusters in the presence of calcium, while it remained monomeric in its absence (Fig 2A). The line scan in Fig 2A' demonstrates that the heights of the particles are 2-4nm and the diameter is about 20nm. These dimensions are in good agreement with the elongated monomer structure determined by SAXS in the absence of calcium. The aggregation of DMP1 in the presence of calcium is shown in the line analysis Fig2C'. Similar results were obtained with the 57 kDa proteolytic fragment from native DMP1 (Fig 2D & E). Phosphate analysis indicated that the 57 kDa fragment contained 41 phosphates (24), suggesting that that both recombinant DMP1 and the native protein could undergo self-assembly in the presence of calcium prior to the induction of biomineralization. The discrepancy observed in the size of the native protein and the recombinant protein is due to the folding pattern as recombinant proteins are folded differently when compared with the native protein. Overall, the AFM images support the SAXS data analysis and interpretation.

In order to further understand the interaction between DMP1 and *de-novo* calcium phosphate nanoclusters in solution, AFM imaging was conducted in pseudophysiological buffer (10 mM HEPES, 165 mM NaCl, 2.5 mM $CaCl_2$, 1 mM KH_2PO_4, pH 7.4) in the presence and absence of DMP1. Results from an overnight incubation (37°C) and in the absence of DMP1 demonstrate that calcium phosphate clusters of all sizes were formed in solution under these conditions with a high proportion of large aggregates (Fig 3a, b). These results confirm the assumption that physiological buffer is supersaturated with respect to calcium phosphate and can readily precipitate as calcium phosphate microclusters (25). However, when DMP1 (1μM) was introduced to the physiological buffer and incubated (37°C overnight) aggregates were reduced in number. In contrast nanorods with dimensions of approximately 20 nm in diameter and approximately 50 to 150 nm in length were observed under this particular condition. These nanorods are likely composed of a protein-mineral complex (Figure. 3c, d). TEM imaging was used to confirm the structure of the nanoclusters. In this experiment DMP1 (5 μg/ml) was introduced to a buffer (10 mM HEPES, 165 mM NaCl, 5 mM $CaCl_2$, 2 mM KH_2PO_4, pH 7.4) and incubated (37°C overnight). We anticipated that with higher concentrations of DMP1 and calcium and phosphate ions in solution, larger self-assembled structures would form. TEM analysis with enhanced contrast by negative staining, demonstrated the presence of protein microfibrils in solution (Figure. 4a). Further examination revealed that most of these protein fibrils were localized on the surface and sequestered with calcium phosphate particles (Figure. 4b, c). These particles were identified as hydroxyapatite nanocrystals by the characteristic (002) electron diffraction pattern obtained from high resolution TEM analysis and selected area electron diffraction (SAED) pattern depicted the preferred c-axis growth (Figure 4d). Control experiments were also performed without DMP1 under identical conditions or with the same concentration of bovine serum albumin. Under these conditions no protein fibril-apatite nanocrystal composites were apparent and the morphology of apatite formed in BSA solution was similar to calcium phosphate crystals formed in its absence which indicates that there is no specific surface recognition between BSA and the mineral surface (Figure 4e). The buffering action of serum albumin might be due to its weak calcium binding property (26). This data is in good agreement with the previous report which shows serum albumin as an apatite nucleation inhibitor (27). Overall, these results demonstrate that DMP1 can sequester high concentrations of calcium phosphate nanoclusters with a high degree of specificity and molecular recognition mechanisms. We hypothesize that during mineralized matrix formation these preassembled nanophase precursors, containing organic molecules, might be necessary for ordered mineral deposition. This observation correlates well with a recent report that states "nanoparticle precursors offer a rich and controllable source material for biomineralization" (28).

DMP1 regulates calcium phosphate precipitation from supersaturated solution

Initial stages in the formation of a biomineral require the presence of an organized template. To characterize this early event, the mineral precipitation assay was conducted as previously described (23). A supersaturated solution (10 mM HEPES, 165 mM NaCl, 5 mM $CaCl_2$, 2 mM KH_2PO_4, 1 mCi/l $^{45}CaCl_2$) in the presence of varying DMP1 concentrations, BSA, or without additives were monitored until the solution reached equilibrium. In the absence of additives, mineral deposition was spontaneous when calcium and phosphate solutions were mixed together. Equilibrium was attained within 3 h with a final calcium concentration (2.2 ± 0.1 mM) in the supernatant, a concentration lower than that found in body fluids (2.5 mM) (Figure. 5a). The addition of DMP1 significantly retarded the mineral precipitation process in solution, especially noticeable during the first three hours, when the calcium concentration of the supernatant was significantly higher than that of the control solution. This trend was found to be concentration dependent, with a higher retention capacity observed at 5 mg/ml DMP1 when compared with 1 mg/ml. Equilibrium was reached within 4 hours at a supernatant concentration of approximately 2.5 ± 0.1 mM for both. In the current study, BSA that was used as a control

also slowed the mineral deposition process, but not as efficiently as DMP1. Based on the above results, we postulate that DMP1 bound newly formed calcium phosphate nuclei in solution with high avidity and thus inhibited the instantaneous precipitation of calcium phosphate. To quantitate the amount of calcium phosphate stabilized by DMP1 in solution, pseudophysiological buffers (165 mM NaCl, 10 mM HEPES, 2.5 mM $CaCl_2$, 1 mM KH_2PO_4) were incubated (37 °C) in the presence or absence of DMP1 (.5 µg/ml) for 1 month. The supernatant was analyzed by SAXS. The scattering intensity of the DMP1 containing calcium phosphate solution is significantly higher than that of the solution without DMP1 (Figure. 5b). By subtracting the scattering contribution of the DMP1 from the background, the scattering intensity from the total calcium phosphate clusters could be determined. The results from the time-resolved calcium phosphate precipitation assay showed that the addition of DMP1 could significantly lower the rate of calcium phosphate precipitation from supersaturated solution when compared to the control. SAXS experiments were also conducted in the long Q range (0.0013-0.068 $Å^1$). Supersaturated calcium phosphate buffer was prepared instantaneously with or without DMP1 (5 µg/ml) and monitored in a time-lapse manner. Results demonstrate that calcium phosphate nanoparticles formed rapidly within 1 min and stabilized within 20 min. However, in the presence of DMP1, we observed marked retardation of calcium phosphate precipitation as nanoparticles and the kinetics was slower as indicated by the scattering intensity (supplementary data). Thus SAXS data confirmed that DMP1 could sequester and stabilize calcium phosphate clusters formed de-novo and that these protein-mineral complexes were suspended as nanoclusters in solution

Discussion

In biomineralization systems such as bone and dentin, uninhibited mineral precipitation from supersaturated solution would override the well-regulated nucleating function of anionic proteins and impair the fine texture of bone crystals. Such a scenario would literally drain the extracellular fluid of its calcium and phosphate content. Therefore, a mechanism is required to prevent the spontaneous formation of calcium phosphate nuclei and subsequent precipitation. Currently, the mechanism of harnessing spontaneous mineral precipitation has been largely ignored.

The initial step in the fabrication of biominerals is the formation of an organized reaction milieu suitable for mineralization. Since soluble macromolecules can influence crystal habit, we first determined the molecular shape of DMP1 in solution and in the presence of calcium using SAXS. SAXS in conjunction with data analysis software is an excellent tool to characterize the conformational states of macromolecules and the growth of nanoparticles in solution (20). This technique can be further exploited to characterize the protein folding process and generate low resolution protein structures in ambient solutions (20).

In this study DMP1 was shown to undergo conformational changes and extensive dimerization upon calcium binding as revealed by the increase in Rg values. The dimerization may be initiated by conformational changes from a random coil to beta-sheet structures and are likely formed by the intermolecular assembly of two C-terminal domains. Presumably calcium binding to phosphate and carboxyl groups on DMP1 reduces the mutual repulsion of negatively charged domains and permits formation of beta sheets. Similar calcium-induced oligomers were formed when specific acidic peptides from DMP1 were immobilized on a solid support (7).

These self–assembled DMP1 fibrils in solution form a structured template, with the presence of a hydrophilic surface comprised of negatively charged aspartic acid and glutamic acid residues at the C-terminus (10). Results from TEM studies show that such an arrangement facilitates sequestration of calcium phosphate nuclei present in supersaturated solution and

form fibrils of protein-mineral complex. Therefore, this negatively charged fibril forms a stable structure by binding with calcium phosphate nanoparticles and protects the nascent mineral nuclei from further growth and precipitation. Specific recognition between DMP1 and the apatite surface might be necessary for the molecular construction of discrete nanoparticle precursors. Such a molecular recognition mechanism could aid in the controlled growth of the nuclei with crystallographic orientation that could play a vital role in controlled bone and dentin calcification. Similar mechanisms have been proposed for the sequestration of calcium phosphate by casein phosphopeptides (29).

The radius of gyration measurement demonstrates that DMP1 could undergo oligomerization in solution and form elongated dimers in the presence of calcium. The low-resolution model obtained in the presence of calcium, depicts a dumb-bell shaped structure with two elongated C-terminal domains wound together and the globular N-terminus located at both ends. This extended domain was assigned a β-sheet conformation, based on our previous study (7). The formation of an elongated molecule could only be brought about by the tandem arrangement of the monomers in such a way that dimerization is facilitated by the C-terminal domain. The oligomerization property of DMP1 might be essential for the formation of ordered templates for binding calcium phosphate nanoparticles.

Further, this study demonstrated that spontaneous precipitation of calcium phosphate particles from a supersaturated solution was found to be slower in the presence of DMP1. Thus, DMP1 could sequester and stabilize newly formed calcium phosphate clusters. During biomineralization, osteoblasts and odontoblasts, the principal cells in bone and dentin formation, actively transport calcium ions toward the site of mineral formation, thereby forming high calcium concentrations at the mineralization front (30). Based on our studies we speculate that after DMP1 is synthesized and secreted by the osteoblasts/odontoblasts, it sequesters calcium phosphate nanoparticles and prevents the precipitation of these salts in the serum. Thus DMP1 could serve dual roles during bone and dentin formation: namely, crystal growth inhibition and prevention of further calcium phosphate nuclei growth by stabilizing these nanoclusters and at the same time promoting controlled mineral nucleation when immobilized specifically on a self-assembled collagen template (Fig 6).

Conclusion

The current study suggests that the formation of calcified tissues is a highly regulated process. To achieve a hierarchically ordered mineralized texture, at least two regulatory mechanisms are required namely: (1) Initiation of apatite nucleation at specific sites on the collagen fibril crystal growth and (2) Prevention of uninhibited crystal growth and formation in areas in which mineralization is not desirable. We have demonstrated that macromolecules like DMP1 present in the organic matrix can undergo conformational change and form a pre-organized template. The initiation of apatite nucleation is highly dependent upon the formation of a pre-organized template and molecular recognition functions. Knowledge of such mechanistic approaches would be useful in studying calcification mechanisms.

Supplementary Material

Refer to Web version on PubMed Central for supplementary material.

Acknowledgement

Abbreviations and Textual Footnotes

DMP 1, Dentin Matrix Protein 1; AFM, Atomic Force Microscopy; TEM, Transmission Electron Microscopy; SAXS, Small angle X-ray scattering analysis; BSA, Bovine serum albumin.

Reference

1. Weiner S, Wagner HD. The Material Bone: Structure-Mechanical Function Relations. Annu. Rev. Mater. Sci 1998;28:271–298.

2. Gao H, Ji B, Jager IL, Arzt E, Fratzl P. Materials become insensitive to flaws at nanoscale: Lessons from nature. Proc. Natl. Acad. Sci. U. S. A 2003;100:5597–5600. [PubMed: 12732735]

3. Jager I, Fratzl P. Mineralized Collagen Fibrils: A Mechanical Model with a Staggered Arrangement of Mineral Particle. Biophys. J 2000;79:1737–1746. [PubMed: 11023882]

4. Blumenthal NC, Posner AS. Hydroxyapatite: Mechanism of formation and properties. Calc. Tiss. Res 1973;13:235–243.

5. Eanes ED, Gillessen IH, Posner AS. Intermediate states in the precipitation of hydroxyapatite. Nature 1965;208:365–367. [PubMed: 5885449]

6. Hunter GK, Hauschka PV, Poole AR, Rosenberg LC, Goldberg HA. Nucleation and inhibition of hydroxyapatite formation by mineralized tissue proteins. Biochem. J 1996;317:59–64. [PubMed: 8694787]

7. He G, Dahl T, Veis A, George A. Apatite nucleation in-vitro self assembled dentin matrix protein. Nat. Mater 2003;2:552–558. [PubMed: 12872163]

8. Xiao S, Yu C, Chou X, Yuan W, Wang Y, Bu L, Fu G, Qian M, Yang J, Shi Y, Hu L, Han B, Wang Z, Huang W, Liu J, Chen Z, Zhao G, Kong X. Dentinogenesis imperfecta 1 with or without progressive hearing loss is associated with distinct mutations. DSPP, Nature Genet 2001;27:201–204.

9. Orme CA, Noy A, Wierzbici A, McBride MT, Grantham M, Teng HH, Dove PM, DeYoreo. Formation of chiral morphologies through selective binding of amino acids to calcite surface steps. Nature 2001;411:775–779. [PubMed: 11459051]

10. George A, Sabsay B, Simonian PA, Veis A. Characterization of a novel dentin matrix acidic phosphoprotein. Implications for induction of biomineralization. J. Biol. Chem 1993;268:12624–12630. [PubMed: 8509401]

11. Qin C, Xiaoling S, Jarrod J, George Anne, Ramachandran Amsaveni, Jeffrey PG, William TB. A comparative study of sialic acid-rich in rat bone and dentin. Eur. J. Oral. Sci 2001;109:133–141. [PubMed: 11347657]

12. George A, Silberstein R, Veis A. In-situ hybridization shows DMP1 (AG1) to be developmentally regulated dentin specific protein produced by mature odontoblasts. Connect. Tissue Res 1995;33:67–72. [PubMed: 7554964]

13. Kamiya N, Takagi M. Immunohistochemistry of chondromodulin-1 in the human intervertebral discs with special reference to the degenerative changes. Histochem. J 2001;33:545–552. [PubMed: 12005026]

14. He G, George A. Dentin Matrix Protein 1 Immobilized on Type I Collagen Fibrils Facilitates Apatite Deposition *in Vitro*. J. Biol. Chem 2004;279:11649–11656. [PubMed: 14699165]

15. Narayanan K, Ramachandran A, Hao J, He G, Park KW, Cho M, George A. Dual Functional Roles of Dentin Matrix Protein 1. Implications in Biomineralization and gene transcription by activation of intracellular Ca^{2+} store. J. Biol. Chem 2003;278:17500–17508. [PubMed: 12615915]

16. He G, Dahl T, Veis A, George A. Dentin matrix protein 1 initiates hydroxyapatite formation in vitro. Connect. Tissue Res 2003;44(Suppl1):240–245. [PubMed: 12952204]

17. Srinivasan R, Chen B, Gorski JP, George A. Recombinant expression and characterization of dentin matrix protein 1. Connect. Tissue Res 1999;40:251–258. [PubMed: 10757113]

18. Guinier A. La diffraction des rayons X aux tres petits angels : application a 1' etude de phenomenes ultramicroscopiques. Ann. Phys. (Paris) 1939;12:161–237.

19. Svergun DI. Determination of the regularization parameter in indirect-transform methods using perceptual criteria. J. App. Crystallog 1992;25:495–503.

20. Koch MH, Vachette P, Svergun DI. Small angle scattering: a view on the properties, structures and structural changes of biological macromolecules in solution. Q. Rev. Biophys 2003;36:147–227. [PubMed: 14686102]

21. Svergun DI, Petoukhov MV, Koch MHJ. Determination of Domain Structure of Proteins from X-Ray Solution Scattering. Biophys. J 2001;80:2946–2953. [PubMed: 11371467]

22. Volkov VV, Svergun DI. Uniqueness of *ab initio* shape determination in small-angle scattering. J. Appl. Crystallog 2003;36:860–864.

23. Schinke T, Amendt C, Trindl A, Poschke O, Muller-Edterl W, Jahnen-Dechent W. The Serum Protein α_2-HS Glycoprotein/Fetuin Inhibits Apatite Formation *in vitro* and in Mineralizing Calvaria Cells: A Possible role in mineralization and calcium homeostasis. J. Biol. Chem 1996;271:20789–20796. [PubMed: 8702833]

24. Qin C, Brunn JC, Cook RG, Orkiszewski RS, Malone JP, Veis A, Butler WT. Evidence for the Proteolytic Processing of Dentin Matrix Protein 1 Identification and characterization of processed fragments and cleavage site. J. Biol.Chem 2003;278:34700–34708. [PubMed: 12813042]

25. Eanes ED. The interaction of supersaturated calcium phosphate solutions with apatitic substrates. Calcif. Tissue Res 1976;20:75–89. [PubMed: 1260495]

26. Triffitt JT, Owen M. Preliminary studies on the binding of plasma albumin to bone tissue. Calcif. Tissue. Res 1977;23:303–305. [PubMed: 902148]

27. Eanes ED, Hailer AW. Anionic effects on the size and shape of the apatite crystals grown from physiological solution. Calcif. Tissue Int 2000;66:449–455. [PubMed: 10821882]

28. Navrotsky A. Energetic clues to pathways to biomineralization: precursors, clusters, and nanoparticles. Proc. Natl. Acad. Sci 2004;101:12096–12101. [PubMed: 15297621]

29. Little EM, Holt C. An equilibrium thermodynamic model of the sequestration of calcium phosphate by casein phosphopeptides. Eur. Biophys. J 2004;33:435–447. [PubMed: 14735250]

30. Linde A, Lundgren T. From serum to the mineral phase. The role of the odontoblast in calcium transport and mineral formation. Int. J. Dev. Biol 1995;39:213–222. [PubMed: 7626409]
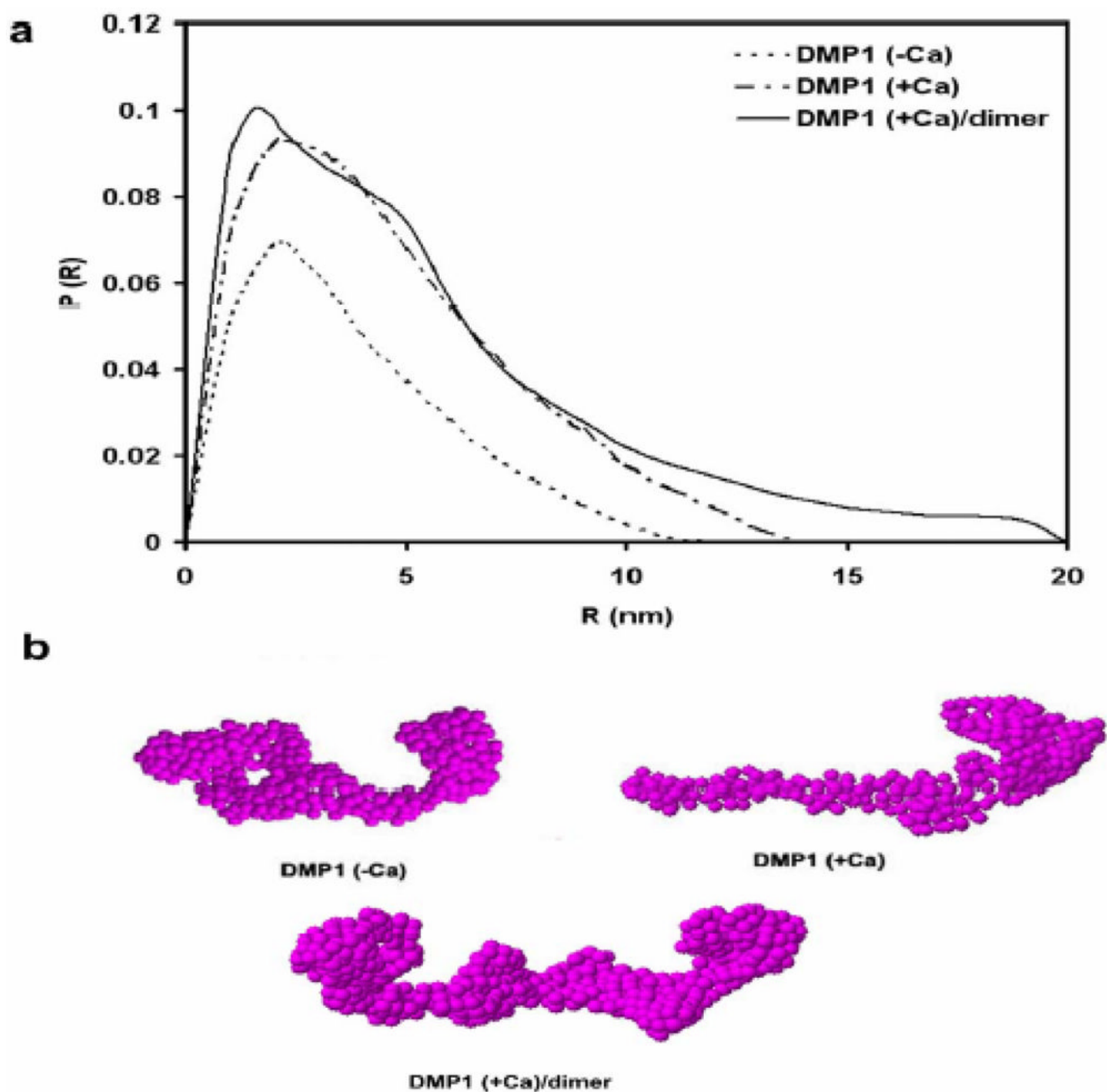
Fig. 1.
Structural Analysis of DMP1 as deduced from small angle X-ray scattering experiments. Changes of distance distribution functions P(R) plots of DMP1 in the presence and absence of calcium ions as computed from time-resolved X-ray scattering patterns (a) and the corresponding low- resolution models determined using GASBOR (b). Calcium binding increased the D_{max} and lead to DMP1 dimerization after 3 min calcium treatment.The P (r) function intensity is reported in arbitrary units.
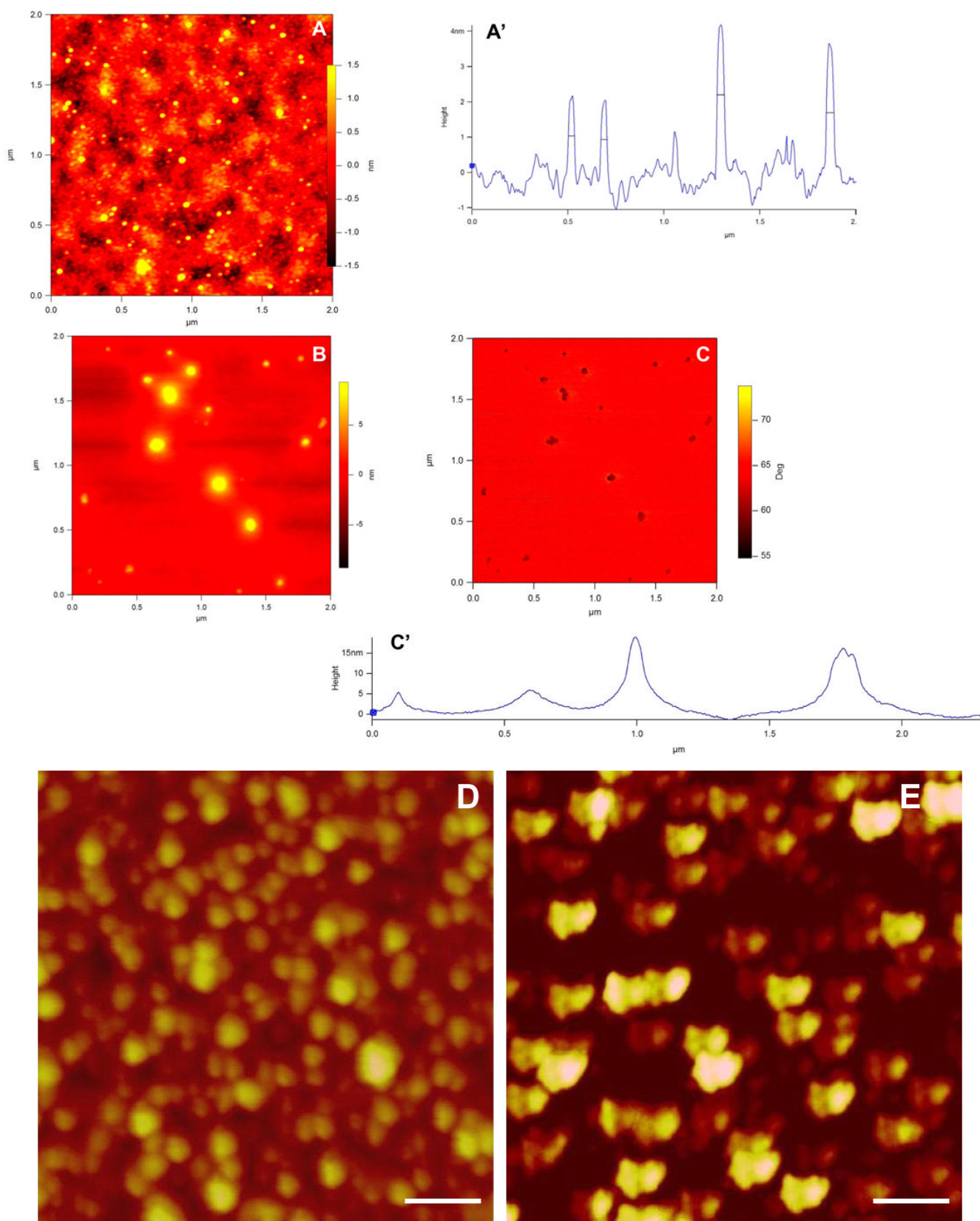
Fig. 2.
Self –assembly of DMP1 as tracked by AFM imaging in tapping mode: A: Topographic image of the monomeric state of recombinant DMP1. A': Line analysis of A (particle size : ∼ 28.2 ± 1.9 nm; n=15). Images of oligomerized dentin in the presence of 2.5 mM Ca^{2+} after overnight incubation. B: Topography (particle size varied from 66.63 to 113.6 nm); C: Corresponding phase image. C': Line analysis from B. .D: Topographic image of the monomeric state of the 57 kDa COOH terminal region of native DMP1; (particle size : ∼ 15nm) (E): Topographic image of oligomerization of the 57 kDa COOH-terminal region of native DMP1 in the presence of 2.5 mM Ca^{2+} after overnight incubation (particle size : ~38 nm). All images were collected at a resolution of 512×512. Scale bars are 75nm.
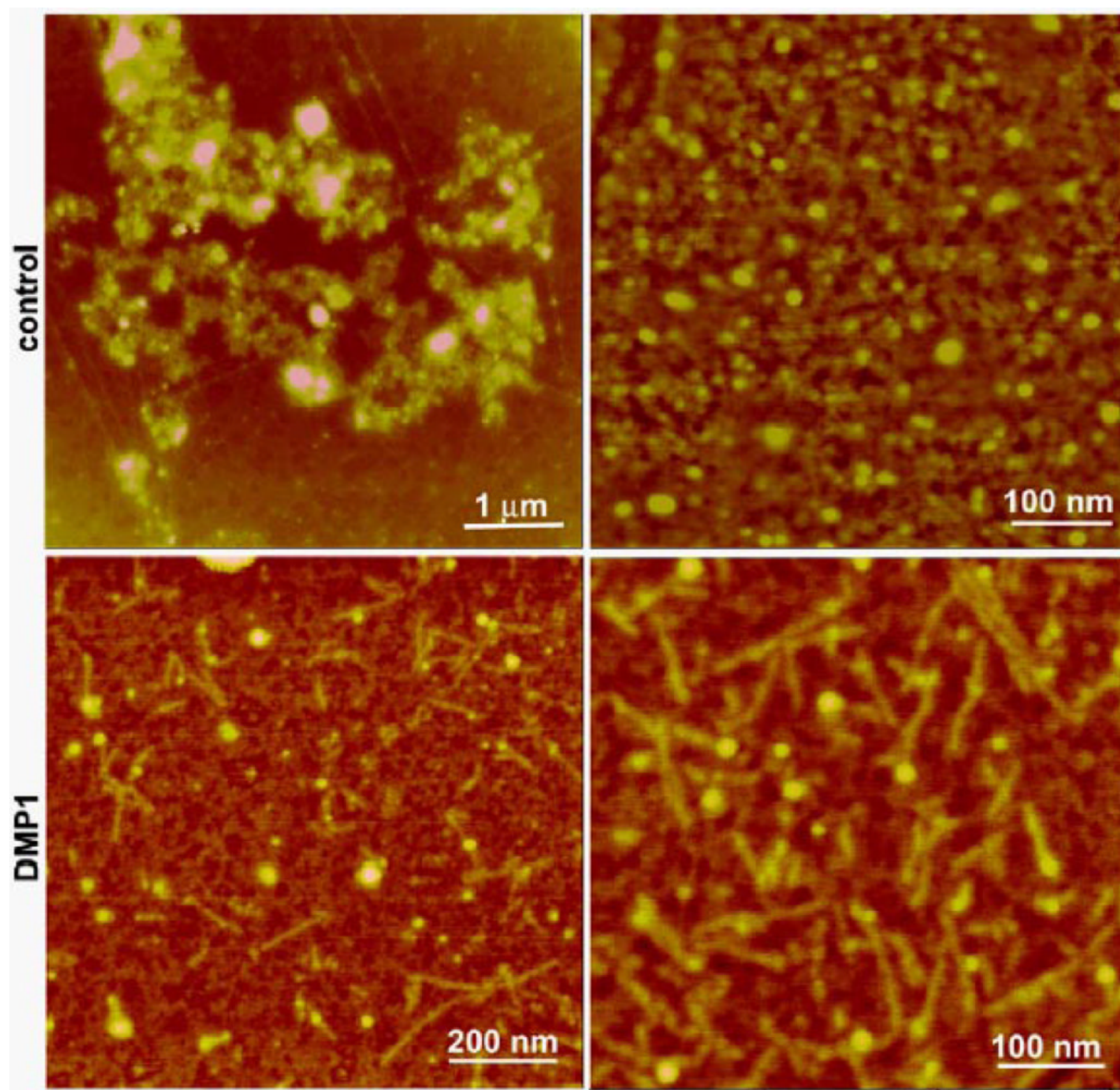
Fig. 3.
Assembly of calcium phosphate clusters in the presence of DMP1 tracked by AFM imaging.
The formation of calcium phosphate nuclei in pseudophysiological buffer and their aggregation
resulted in large agglomerate formation and precipitation (a, b). Addition of DMP1 0.5 μg/ml
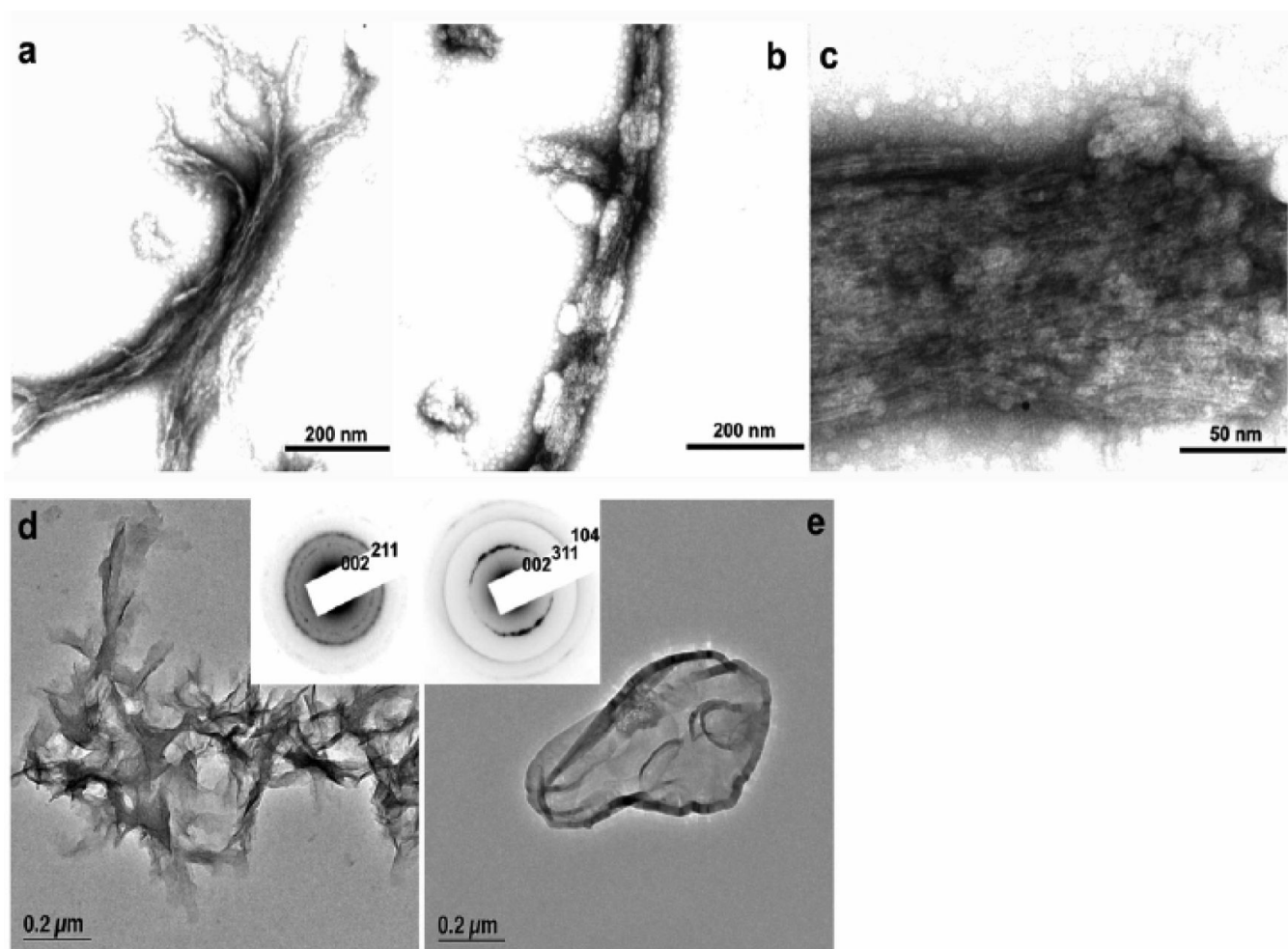promotes the assembly of a protein-mineral complex shaped as nanorods ($\sim 100 \times 20$ nm)
(c,d).

Fig. 4.
Characterization of DMP1-mineral complex formation. TEM analysis demonstrate the presence of DMP1 5 µg/ml DMP1) fibrils in buffer (10 mM HEPES, 165 mM NaCl, 5 mM CaCl$_2$, 2 mM KH$_2$PO$_4$, pH 7.4) (a). Most of the fibrils were decorated with mineral particles (b). At higher magnification, mineral nuclei were observed to be trapped in the protein fibrils (c). The same sample was analyzed by high resolution TEM. The corresponding selected area diffraction pattern showed that the embedded minerals are hydroxyapatite nanocrystals (d). No fibrils were observed in controls containing BSA (5 µg/ml) (or without protein). Only microscale hydroxyapatite was precipitated in the control solutions (e). Insets (d, e) are the corresponding selected area diffraction patterns.
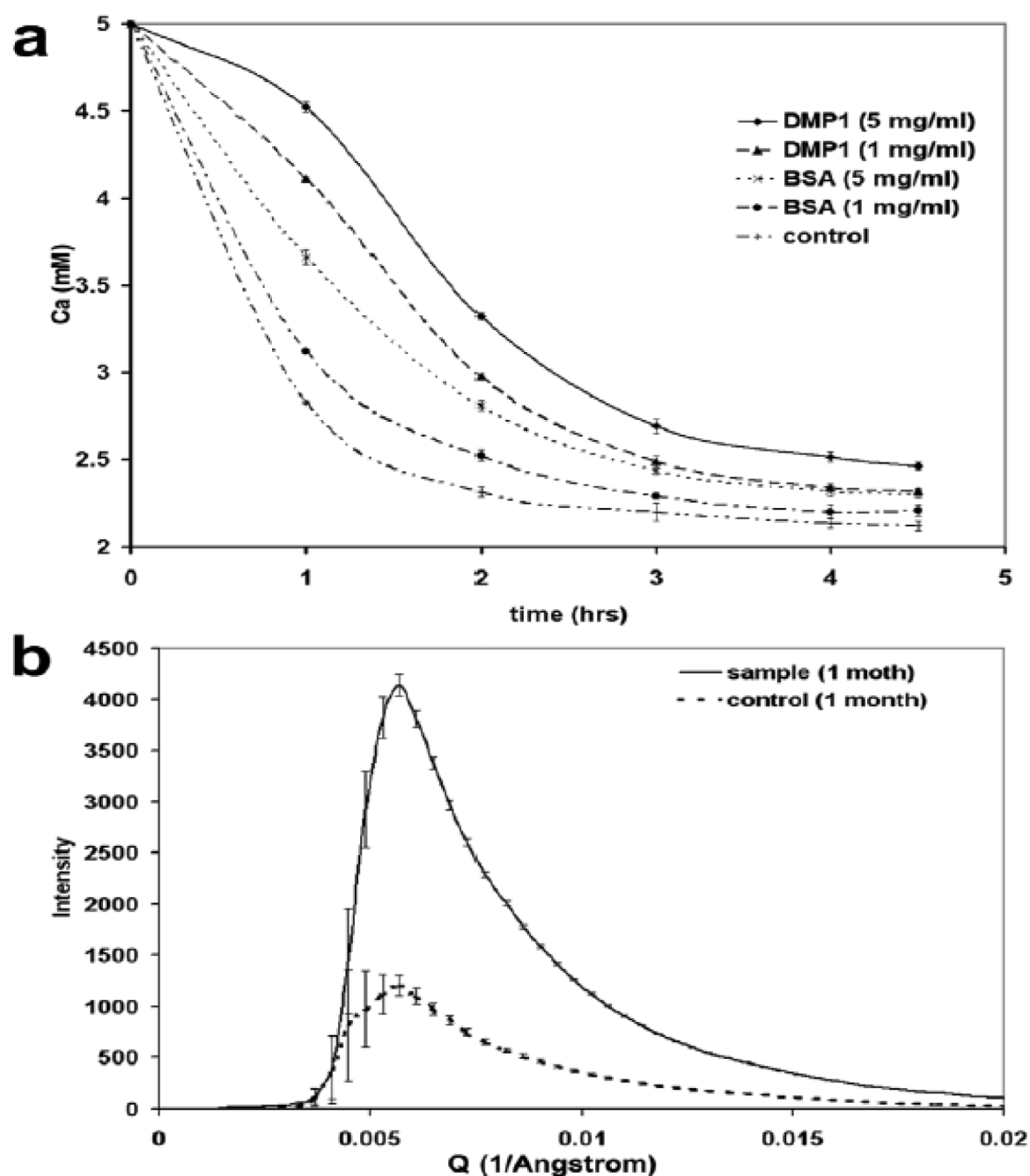
Fig. 5.
DMP1 can inhibit spontaneous mineral precipitation by tethering calcium phosphate nuclei. The calcium phosphate precipitation assay showed that DMP1 can temporarily inhibit spontaneous calcium phosphate precipitation from supersaturated calcium phosphate solution (a). Note, BSA also promotes calcium homeostasis but not as efficiently as DMP1. (b) SAXS analysis indicated that scattering intensity is higher in a buffer (10 mM HEPES, 165 mM NaCl, 5 mM $CaCl_2$, 2 mM KH_2PO_4, pH 7.4) containing DMP1 0.5 µg/ml than that in the absence of DMP1 after 1 month incubation, which suggests that a great number of calcium phosphate nanoclusters were present in the DMP1 containing solution than in the control.
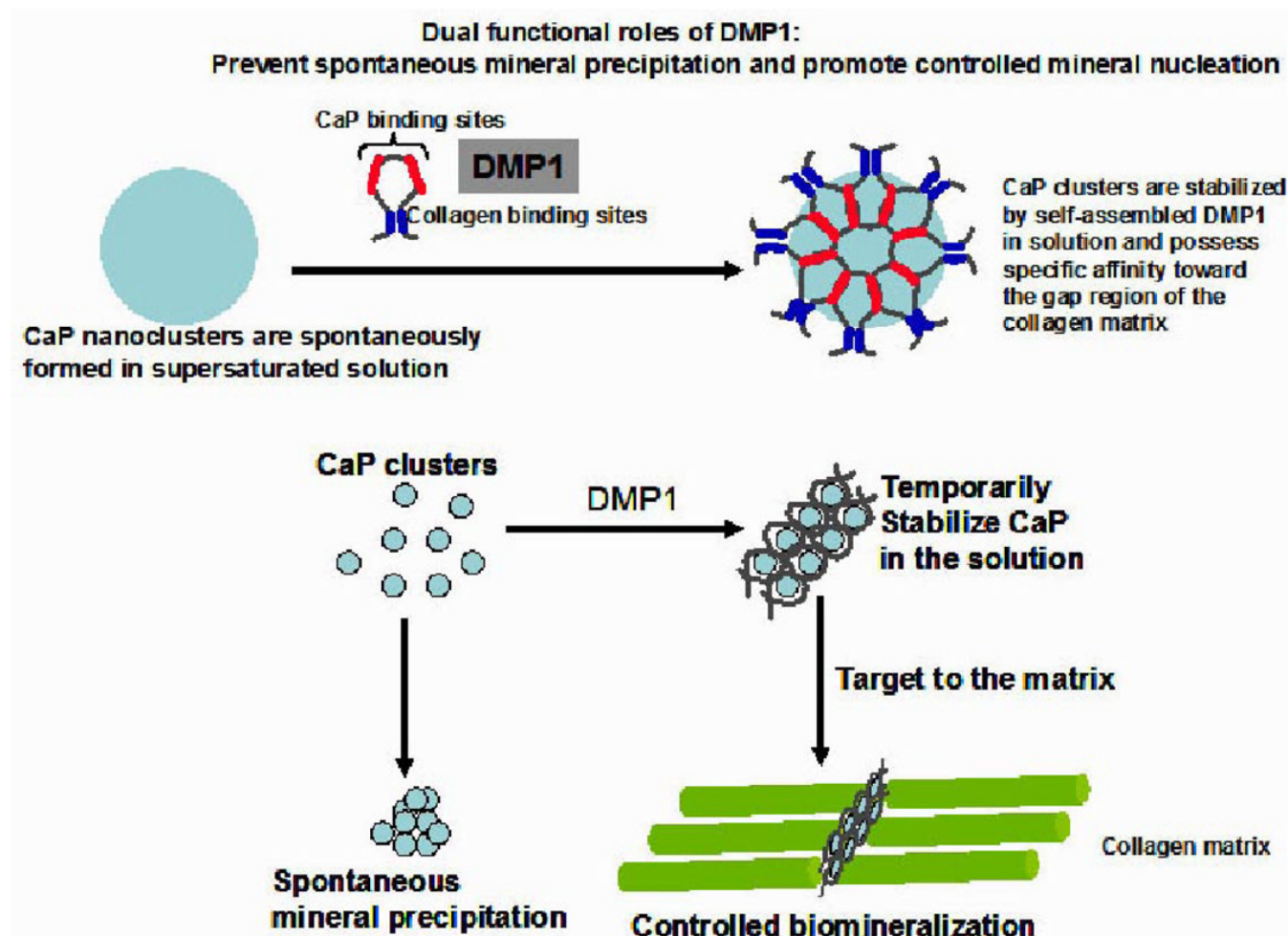
Fig. 6.
Proposed model for the dual functional role of DMP1: Based on experimental data, the model demonstrates that DMP1 can inhibit spontaneous mineral precipitation and promote controlled mineral nucleation on a collagenous template (14).